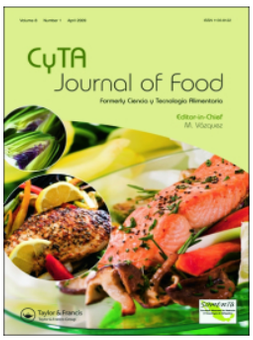

CyTA - Journal of Food

ISSN: (Print) (Online) Journal homepage: https://www.tandfonline.com/loi/tcyt20

Fabrication and characterization of edible films from *acha* (*Digitalia exilis*) and *iburu* (*Digitalia iburua*) starches

Buliyaminu Adegbemiro Alimi, Tilahun Seyoum Workneh & Fortune Abidemi Femi

To cite this article: Buliyaminu Adegbemiro Alimi, Tilahun Seyoum Workneh & Fortune Abidemi Femi (2021) Fabrication and characterization of edible films from *acha* (*Digitalia exilis*) and *iburu* (*Digitalia iburua*) starches, CyTA - Journal of Food, 19:1, 493-500, DOI: 10.1080/19476337.2021.1917667

To link to this article: https://doi.org/10.1080/19476337.2021.1917667

Published online: 19 May 2021.

CYTA – JOURNAL OF FOOD
2021, VOL. 19, NO. 1, 493–500
https://doi.org/10.1080/19476337.2021.1917667

Fabrication and characterization of edible films from *acha* (*Digitalia exilis*) and *iburu* (*Digitalia iburua*) starches

Buliyaminu Adegbemiro Alimi[a,b], Tilahun Seyoum Workneh[a] and Fortune Abidemi Femi[b]

[a]Bioresources Engineering, School of Engineering, College of Agriculture, Engineering and Science, University of KwaZulu-Natal, Scottsville, South Africa; [b]Department of Food Science and Technology, School of Agriculture and Agricultural Technology, Federal University of Technology, Minna, Nigeria

ABSTRACT

Some properties of biodegradable edible films developed from starches of *acha* (*Digitalia exilis*) and *iburu* (*Digitalia iburua*), with glycerol as plasticizer, were evaluated and compared. Scanning electron microscope revealed that *acha* starch film (ASF) had rougher surface with larger size spores. Both films showed similar crystallinity pattern made up of A-type pattern of cereal starch as backbone and process induced V_H-crystals. FTIR spectroscopy revealed the traces of some non-starch components in the films matrices. Both films had near-equal thickness (≈0.02 mm). However, *iburu* starch film (ISF) exhibited higher density, swelling power, water solubility and mechanical resistant while ASF gave higher water vapor permeability. Both films maintained their integrity during water solubility testing period. ISF had significantly ($p < .05$) higher transparency (97.08%) while ASF had higher a^* (−0.06) and b^* (1.81) values. Films from the starches exhibited promising characteristics that could place them as good materials for different packaging requirements.

ARTICLE HISTORY
Received 11 February 2021
Accepted 10 April 2021

KEYWORDS
Cereal crops; *acha*; starch films; packaging; *iburu*; optical properties

PALABRAS CLAVE
Cultivos de cereales; acha; películas de almidón; envases; iburu; propiedades ópticas

Fabricación y caracterización de películas comestibles a partir de almidones de acha [mijo] (*Digitalia exilis*) e iburu (*Digitalia iburua*)

RESUMEN

El presente estudio se propuso evaluar y comparar algunas propiedades de las películas comestibles biodegradables elaboradas a partir de almidones de acha (*Digitalia exilis*) e iburu (*Digitalia iburua*), utilizando glicerol como plastificante. El microscopio electrónico de barrido permitió constatar que la película de almidón de acha (ASF) posee una superficie más rugosa, presentando esporas de mayor tamaño. Ambas películas muestran un patrón de cristalinidad similar, conformado por un patrón de tipo A del almidón de cereal como columna vertebral y por cristales V_H inducidos por el proceso. Mediante la espectroscopia FTIR se comprobó la presencia de algunos componentes no relacionados con el almidón en las matrices de las películas. Ambas películas tienen un grosor casi igual (≈0.02 mm). Sin embargo, la película de almidón iburu (ISF) presenta mayor densidad, poder de hinchamiento, solubilidad en agua y resistencia mecánica, mientras que la ASF posee mayor permeabilidad al vapor de agua. Ambas películas mantuvieron su integridad durante el periodo de pruebas de solubilidad en agua. La ISF mostró una transparencia significativamente mayor ($p < .05$) (97.08%), mientras que la ASF registró valores más altos de a* (−0.06) y b* (1.81). En conclusión, las películas de los almidones poseen características prometedoras que podrían situarlas como buenos materiales para diferentes requerimientos de envasado.

1. Introduction

Interest in the development of films with good barrier properties against moisture and gas continues to wax stronger. The new thrust is in the development of films from renewable and biodegradable macromolecules such as starch and protein (Jafarzadeh et al., 2020). Films from these sources have advantages in food and pharmaceutical applications over conventional synthetic plastic films. Their principal advantages are eco-friendliness, relative cheapness and safety to human health (Dang & Yoksan, 2016; Mei et al., 2020). They may also be consumed along with the foods and drugs they wrap. Films from these natural biopolymer sources have been reported to provide good structural protection to the food and pharmaceutical products. They are also known to maintain the original quality and aesthetic of the wrapped products because they are colorless, odorless and tasteless (Akman et al., 2021). However, starch, because of its dominant attributes that impart positively on the structural and functional properties of the resulting films, is the most patronized base material of all the renewable sources for the development of edible films (Yildirim-Yalçin et al., 2019).

Major appeals of starch are its abundance availability, ease of extraction, high yield and excellent functional properties that enhance its compatibility, and therefore, its applicability in food and pharmaceutical systems (Alimi et al., 2016). Edible films have been developed from major and popular starch sources such as corn, cassava and plantain. Competition between different industries for starch is putting serious pressure on the known sources. The effects

CONTACT Buliyaminu Adegbemiro Alimi, bun5574@yahoo.com; baalimi@gmail.com Bioresources Engineering, School of Engineering, College of Agriculture, Engineering and Science, University of KwaZulu-Natal, Private Bag X01, Pietermaritzburg, Scottsville 3209, South Africa

of this include limited availability to satisfy the industries and high purchasing cost of starch because of heavy demand. It is therefore, necessary to explore other sources of starch for specific industrial applications. Attention is now shifting to the exposition of potentials of starch from underutilized sources with good starch content.

Acha (*Digitalia exilis*) and *iburu* (*Digitalia iburua*) are in the class of underutilized starch-rich cereal crops (Alimi & Workneh, 2018). Their excellent agronomic, ecological and food values that place them above some well-known cereal crops have been reported in literature (Arueya & Oyewale, 2015). These include excellent performance on low inputs, early maturation, high starch yield and economic returns. Others are presence of sulphur amino acids (known for its role in proper functioning of the heart and nerve transmission) in considerable amount in their starches and its perceived nutraceutical potential (basis for its use in some culture to manage diabetes). Several new products have been developed from *acha* and *iburu* starches and flours (Jideani & Jideani, 2011). However, there is no information on the development of edible films from the starches of these important cereal crops.

Literature is replete with the development and characterization of edible films from some major cereal and other starch rich crops. Reports from the studies revealed that properties of base starch had greater reflection on the final characteristics of the resulting films (Daudt et al., 2016). It is, therefore, important to determine the properties of films from specific starch sources on their merit to determine their applications in food and drug packaging systems. Hence, the objectives of this study were to develop and characterize edible films from *acha* and *iburu* starches.

2. Materials and methods

2.1. Experimental materials

Acha and *iburu* were obtained from a market in Kano metropolis, Nigeria. Alkaline (sodium metabisulphite) steeping method reported by Arueya and Oyewale (2015) was used to extract starch. Protein was separated from starch by toluene emulsification. The resulting starch was dried in hot air oven at 45°C for 24 h. Glycerol (1, 2, 3-propanetriol glycerin. G49776) that was supplied by Sigma-Aldrich Pty Ltd, Johannesburg, South Africa was used as plasticizer.

2.2. Film preparation

Casting method as described by Daudt et al. (2016) was used to prepare edible films. Starch (3 g) was dispensed into solution of 2.0 mL of glycerol in 100 mL distilled water. The suspension was heated with continuous magnetic stirring (to eliminate bubbles and ensure uniform filmogenic solutions) on hot plate at temperature of 85°C until colorless and viscous film forming solutions (FFS) was formed (approximately 35 min). The FFS were left to cool. Thirty grams (30 g) of the FFS were weighed into uniform size circular acrylic non-sticky plates for even thickness and dried in hot air convective oven at 40°C for 24 h. Carefully peeled dry films were cured and held in a controlled temperature and humidity chamber (CTS model C-40/100, Hechingen, GmBH) at 25°C and 58% relative humidity for 72 h until analysis.

2.3. Scanning electron micrograph

Dried film samples were fractured into small fragments with tweezers. The fragments were mounted on stubs with the aid of double-sided tapes. Coating of the surface of the films with thin layer of gold was done using EIKO IB-3 sputter ion coater (EIKO Engineering, Hitachinaka, Japan). Microstructure of the films was captured as described by Shaili et al. (2015) using scanning electron microscope (EVO LS 15, ZEISS International, Oberkochen, Germany).

2.4. X-ray diffraction

X-ray diffractometer (D8 Advance, BRUKER AXS, Karlsruhe, Germany) operating at Bragg angle (2Θ) range of 3° to 40°, scan step of 0.035° and step time of 0.5 s, and generator settings of 40 kV and 40 mA was used to capture the diffraction patterns of the dried film samples. Eva software (BRUKER, Germany) was used to obtain multipeak fittings to get integrated areas of crystalline (*Ac*) and amorphous (*Aa*) peaks. Crystallinity index (CI) was calculated thus:

$$CI = \frac{100 \times Ac}{(Ac + Aa)} \tag{1}$$

2.5. Infrared spectroscopy

Infrared spectra of the films were obtained using the procedure described by Alimi and Workneh (2018) with the use of a Fourier Transform Infrared (FTIR) spectrometer (Spectrum 100 series, Perkin Elmer, Beaconsfield, UK) in the wavelength range of 4000–380 cm^{-1} at spectra resolution of 4 cm^{-1}.

2.6. Thickness and density

The thickness of the films was measured with metric micrometer screw gauge (0–25 mm, 0.01 mm diameter). The measurement was taken at five (5) random points in each of the film samples.

Weights of 30 × 30 mm^2 dimension film samples were taken. Film density was calculated as the ratio of weight of the film per unit volume.

2.7. Swelling power and water solubility

Film samples (900 mm^2 each) were dried in convective hot air oven at 80°C for 48 h to determine their initial dry matter. They were left to cool and weighed (w_o). This was followed by immersion (separately) in 25 mL distilled water in beakers for 24 h in the laboratory. The distilled water was poured out and the films were carefully removed from the beakers. Non-shredding adsorbent paper was used to remove surface water from the films and their new weights was taken (w_1). The films were then transferred into oven for drying at 85°C. Their weights (w_2) were periodically checked until constant. Swelling power (SP) and water solubility (WS) were calculated as follow.

$$SP = \left[\frac{w_1 - w_0}{w_0}\right] \tag{2}$$

$$WS = \left[\frac{w_0 - w_2}{w_0}\right] \quad (3)$$

2.8. Water vapor permeability

Water vapor permeability (WVP) of the films was determined using ASTM E96 desiccant method (Arezoo et al., 2020). Film samples were placed in desiccator containing silica gel for at least five days to equilibrate. They were cut into circular sheets of 46 mm diameter, sealed with the aid of silicone on circular mouth glass cups containing silica gel and the weights noted. The assemblages were placed in a desiccator along with a 50 mL eaker of distilled water. Weight increase was observed periodically until no further increase over five checking. WVP was calculated thus.

$$\text{WVP} = \left[\frac{xh}{A\Delta P}\right] \quad (4)$$

Where: x, h, A and ΔP are the gradient of weight increase with time (g/s), thickness of the film (m), film surface area (m^2) and vapor pressure difference across the film (Pa), respectively.

2.9. Strength of the films

Puncture test using a texture analyzer (TA.XT2, Stable Micro System Ltd, Surrey, UK) was deployed to determine the strength of the films. The test was conducted according to ASTM standard method D3882-18 (ASTM, 2018). Film samples were cut into discs of 60 mm diameter and mounted firmly unto a cylindrical capsule with circular opening of 34 mm diameter. Cylindrical probe of 3 mm diameter moving at a speed of 1 mm/s penetrated the film. The peak force obtained from force (g)/time (s) graph was the puncture force.

2.10. Optical properties

A colorimeter (Chroma meter CR 400, Konica Minolta, Japan) was used to determine the *Commission Internationale de l'Eclairage* (CIE) *l*, a** and *b** color parameters. The equipment was standardized with a white tile provided by the manufacturer prior to measurements.

A UV–visible spectrophotometer (UV-VIS Optima Scientific, Cape Town, South Africa) was used to determine the transparency (a measure of light transmittance) of the films. The measurement was taken at 560 nm as described by Shittu et al. (2014). The parameter was calculated as below:

$$T_f = 100 * \left[\frac{T_w}{T_0}\right] \quad (5)$$

T_f, T_w and T_o are film transparence, light transmittance through the film and light transmittance without the film, respectively.

Opacity of the films was measured as described by Santacruz et al. (2015). Spectrophotometer mentioned above was used to determine the absorbance of the films at 600 nm. Opacity was calculated as below:

$$\text{Opacity} = \frac{Abs_{600}}{h} \quad (6)$$

Abs_{600} is the absorbance of the film at 600 nm and h is the film thickness

2.11. Data analyses

All analyses were replicated at least twice. Means and standard deviations were reported. Paired samples T-test at 95% confidence level was used to compared the means. Data analyses were conducted using IBM SPSS 20.0 Statistical package.

3. Results and discussion

3.1. Scanning electron micrographs

The scanning electron micrographs of the surface of the *acha* starch film (ASF) and *iburu* starch film (ISF) are shown in Figure 1. They both showed irregular, non-smooth surfaces. The principal factor may be non-homogeneity of the source starch used for the preparation of the films. For instance, the presence of other macromolecules such as protein, lipids and fiber, and their possible interaction with starch to form complexes may cause intermittent disruption in the polymeric network thereby resulting in the development of film with uneven surfaces. Earlier report of Alimi and Workneh (2018) pointed to the heterogeneity in the *acha* and *iburu* starch matrices. This similar factor was reported to be responsible for irregularities observed on the surfaces of films developed from banana and plantain (Pelissari et al., 2013), and *cush cush* yam and cassava starches (Gutiérrez et al., 2015). Furthermore, comparison of the two films revealed that the surface of ASF was rougher with more number of large size pores than ISF. This could imply that *acha* starch has higher concentration of non-starch macromolecules.

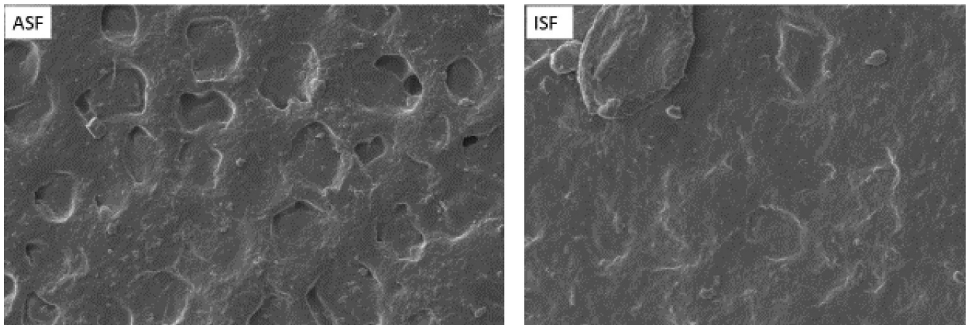

Figure 1. Scanning electron micrograph of surfaces of *acha* and *iburu* starch films (ASF and ISF, respectively) at 500× magnification.

Figura 1. Micrografía electrónica de barrido de las superficies de las películas de almidón de acha e iburu (ASF e ISF, respectivamente) con un aumento de 500×.

3.2. X-ray diffraction

The X-ray diffraction patterns of *acha* and *iburu* starch films are shown in Figure 2. The films from the two starch sources depicted similar crystallinity pattern. They have A-type backbone and V_H crystals. The A-type pattern, characteristic of cereal starch, was obviously from their base starch (Alimi & Workneh, 2018), while the V_H styled crystal characterized by single helical structure was the result of stress during thermal processing (Alimi et al., 2017b).

Iburu starch film had higher crystallinity as shown by its higher crystallinity index (Table 1). This can be partially explained with the observation in Figure 2. Though ASF has higher intensity, but it possesses larger peak width which implies higher amorphous area which could affect its crystallinity. This can be the effect of more presence of other components aside starch, such as protein, fiber and lipids, in *acha* film matrix. Presence of such components have been reported to inhibit retrogradation of amylose during film formation, thus, limiting the prominence of amylopectin (Pelissari et al., 2013). Another line could be the crystallinity potential of the base starch. Alimi and Workneh (2018) had reported that native *iburu* starch had higher crystallinity index than native *acha* starch. The study inferred that the higher CI of *iburu* starch was an indication of its higher amylopectin content; since amylopectin content in a starch is directly related to its crystallinity (Hizukuri et al., 1983).

3.3. FTIR spectra

The FTIR spectra of *acha* and *iburu* starch films (Figure 3) were obtained to identify and classify the interactions taking

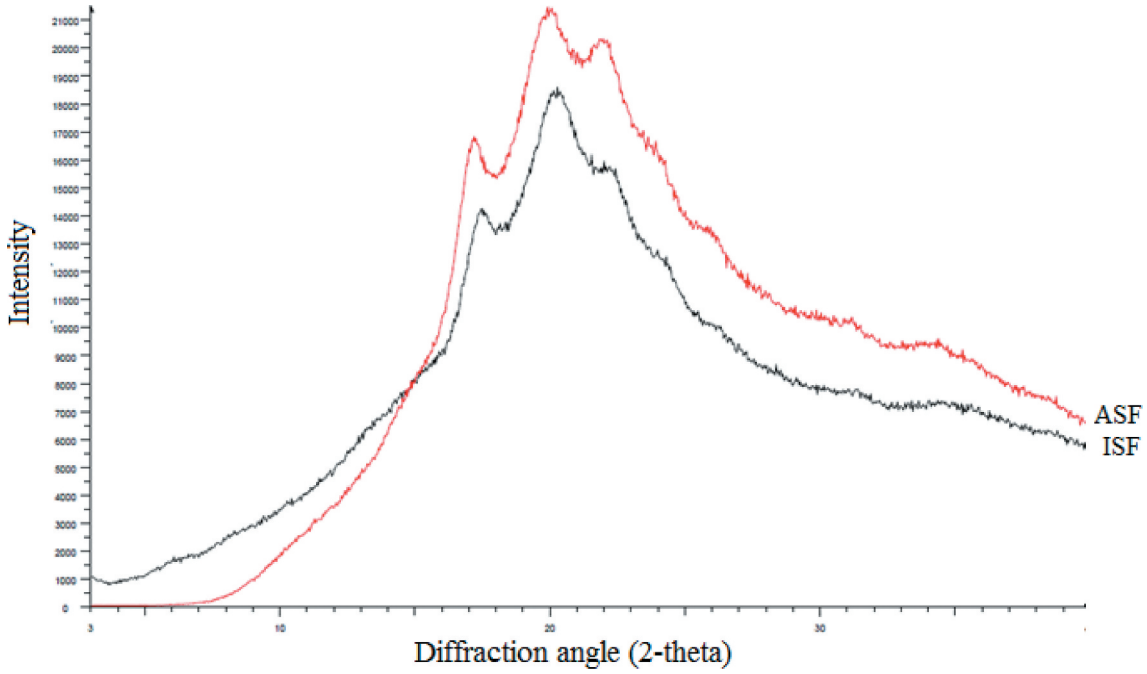

Figure 2. X- ray diffraction patterns of *acha* and *iburu* starch films (ASF and ISF, respectively).

Figura 2. Patrones de difracción de rayos X de las películas de almidón de acha e iburu (ASF e ISF, respectivamente).

Table 1. Functional, mechanical and optical properties of ASF and ISF.

Tabla 1. Propiedades funcionales, mecánicas y ópticas de ASF e ISF.

Properties	ASF	ISF	*P*
Thickness (mm)	0.02 ± 0.0014	0.02 ± 0.005	0.961
Density (g/cm^3)	1.55 ± 0.243	1.93 ± 0.503	0.969
SP (%)	93.16 ± 5.864	99.51 ± 12.490	0.554
WS (%)	21.24 ± 1.997	23.26 ± 1.820	0.993
WVP (10^{-8} g/m s Pa)	1.77 ± 0.113	1.93 ± 0.128	0.154
Puncture force (N)	2.13 ± 0.145	2.44 ± 0.304	0.154
Force at target (N)	0.040 ± 0.003	0.043 ± 0.011	0.123
Transparency (%)	89.19 ± 2.479	97.08 ± 1.554	0.829
Opacity (m^{-1})	4.08 ± 0.227	3.84 ± 0.480	0.914
*l**	37.74 ± 0.106	37.94 ± 0.021	0.000
a*	−0.06 ± 0.021	−0.16 ± 0.000	ND
b*	1.81 ± 0.007	0.53 ± 0.007	0.000

Mean ± SD. Except *l**, *a**, *b** which were repeated twice, other experiments were conducted in triplicate.

ASF: *acha* starch film; ISF: *iburu* starch film; p: level of significance; SP: swelling power; WS: water solubility; WVP: water vapor permeability; *l**: Lightness index; a*: Red-green index; b*: Yellow-blue index; ND: not displayed by the statistical software.

Media ± SD. Excepto l*, a*, b* que se repitieron dos veces, los demás experimentos se realizaron por triplicado.

ASF: película de almidón de acha; ISF: película de almidón de iburu; p: nivel de significación; SP: poder de hinchamiento; WS: solubilidad en agua; WVP: permeabilidad al vapor de agua; *l**: índice de luminosidad; a*: índice rojo-verde; b*: índice amarillo-azul; ND: no mostrado por el *software* estadístico.

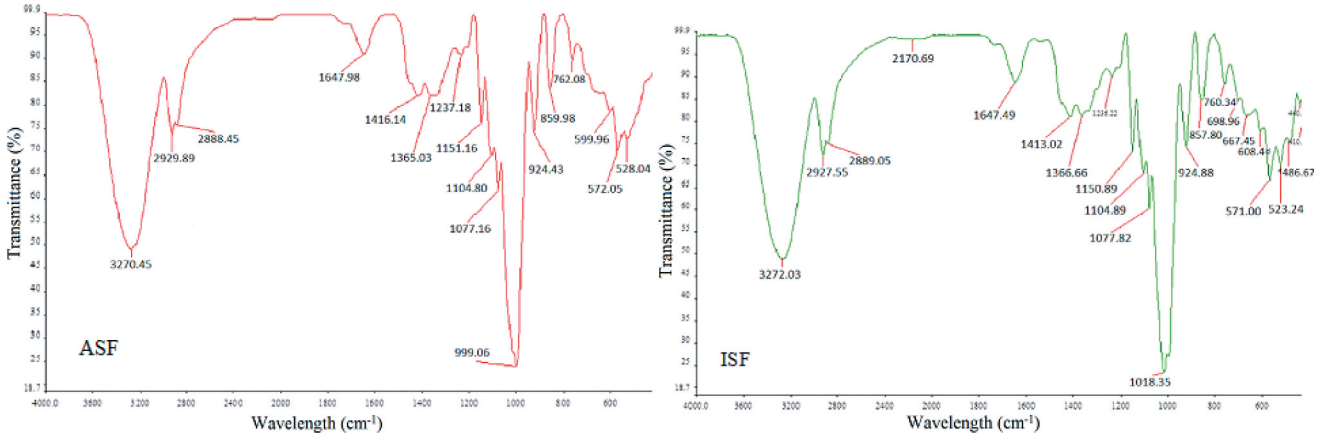

Figure 3. FTIR spectra of *acha* and *iburu* starch films (ASF and ISF, respectively).

Figura 3. Espectros FTIR de las películas de almidón de acha e iburu (ASF e ISF, respectivamente).

place in the film matrices. Spectra of both films showed similar infrared (IR) transmittance patterns. The two most prominent peaks were at 3270.45; 3272.03 cm^{-1} (ASF; ISF, respectively) and 999.06; 1018.35 cm^{-1} (ASF; ISF, respectively). The transmittance band at about 3270 cm^{-1} were the results of hydroxyl bond stretching resonance. They were within the region (3000–3600 cm^{-1}) assigned for the transmittance of energy by hydroxyl groups (Zhang & Han, 2006) and indicated contribution of water molecules to the film structures (Alimi & Workneh, 2018). The prominent bands at 999.06–1018.35 cm^{-1} gave information on the relative degree of crystallinity between the films (Van Soest et al., 1995). The bands within this region reflect amorphous-crystalline transition (Bergo et al., 2010). In this study, the signature band of ISF (1018.35 cm^{-1}) in the region was at higher wavelength. This suggests that ISF was more crystalline than ASF.

Peak bands within the region 2800–3000 cm^{-1} were for CH bond stretching and their intensities were the results of the quantity of amylose and amylopectin in the film matrices. Higher transmittance band indicates lower amylose content and vice-versa (Kizil et al., 2002). The bands identified at about 1647 and 1366 cm^{-1} for both films correspond to amide I and amide III groups of protein, respectively. The detection of these bands indicated the presence of trace proteins from base starch. Bands in these regions were detected in *pinhão* starch films (Daudt et al., 2016), plantain flour and starch films (Pelissari et al., 2013) and *achira* flour film (Andrade-Mahecha et al., 2012). The bands at 1416.14 and 1413.02 cm^{-1} for *acha* and *iburu* starch films, respectively, were due to symmetric stretching of carboxylic groups (Van Soest et al., 1995). The transmittance bands at 760.34 and 762.08 cm^{-1} were indicative of the presence of phenolic compounds in the film matrices (Pelissari et al., 2013).

3.4. Thickness and density

There was no significant difference in the thickness of films from the starches of *acha* (20.467 μm) and *iburu* (19.283 μm) as shown in Table 1. The near similar thickness values obtained for the films may be due to non-variation in the casting procedure employed. Similar observation was reported by Müller et al. (2008).

However, despite the same casting procedure employed, ISF had higher, though insignificant ($p < .05$), density (1.93 g/cm^3) than ASF (1.55 g/cm^3). The lower density value of ASF could be due to the higher number of large pores in its microstructure as revealed by scanning electron micrograph. The pores could have created voids that affected mass distribution in the matrix.

3.5. Swelling power and solubility in water

Swelling power and solubility of the films in water are presented in Table 1. Both parameters are indices of hydration capacity of biopolymers (Alimi et al., 2017a). Integrity of the films was intact throughout the swelling power and solubility testing period. This indicated that the major interactions and bonds within the starch matrices of the films did not breakdown and that the soluble components were the monomers and non-starch constituents in the films (Bourtoom & Chinnan, 2008). This is an important factor for consideration in biomedical application because such films would absorb water and bioactive compound while maintaining their integrity and promoting slow release of drugs with less molecular diffusion (Shittu et al., 2014). Solubility is also important in edible packaging for food when the product would be heated before consumption (Bourtoom & Chinnan, 2008). High SP and solubility values obtained for ISF in this study showed that it was more hygroscopic (Pelissari et al., 2013).

3.6. Water vapor permeability

One of the primary functions of biodegradable edible films is to limit moisture diffusion between the wrapped product and its environment. Therefore, it is important to ensure that WVP is kept low in an instance of top need to control environmental conditions. There was no significant difference in WVP of the two films. The WVP results obtained in this study were comparatively lower to what were reported for *pinhão* starch films (Daudt et al., 2016) and rice starch film (Bourtoom & Chinnan, 2008)

3.7. Mechanical strength of the films

Iburu starch film had higher peak force (2.44 N ≈ 246.72 g) and force at target (0.043 N ≈ 4.41 g) than *acha* starch film

(2.13 and 0.04 N (≈217.09 and 4.08 g), respectively) as shown in Table 1. The implication is that ASF was more flexible than ISF. It was deduced from earlier results in this report that ASF had more concentration of non-starch components such as lipid and protein in its matrix. Interactions of lipid and protein are known to enhance flexibility of films (Batista et al., 2005; Liu et al., 2018). Lipid–protein interactions led to creation of intermolecular networks within the matrix. The networks weakened the strong molecular bonds in the film matrix through their lubricating effect as they came in between the molecules (Sanyang et al., 2016). The lubricating effect of vast lipid-protein networks in ASF is the possible reason for its higher flexibility. Similar observation was reported by other authors for mechanical property of biopolymer films (Daudt et al., 2016; Pelissari et al., 2013).

The force–time graphs of the films displayed non-linear increase of force with displacement up to the breaking point (Figure 4). The higher resistance of ISF to break or deformation, represented by its higher puncture force, could be due to its more compact microstructure as previously shown in the scanning electron micrographs of the films in Figure 1. Similar observation was reported by Gutiérrez et al. (2015).

Intending application of films determines its mechanical strength requirement. Highly flexible films find important application in direct fruits and food wrappings while brittle biodegradable films with great resistance to deformation are useful as packaging materials to reinforce food structure.

3.8. Optical properties

Optical properties of packaging materials are important determinants of their visual perception by consumers and eventual acceptability or otherwise (Alimi et al., 2014). Films from the two starch sources had high transparency values (Table 1). This tendency can position both films as good candidates in packaging system where clarity and transparency are of essence. However, ISF had higher transparency value than ASF. Two major factors that could be responsible for the observed difference in their transparency are thickness and sizes of particles (Kampeerapappun et al., 2007). Effect of thickness on the transparency of films in this study was negligible since the thickness of the films did not differ significantly (Table 1). Transparency is a measure of light transmittance through the films. Particles affect film transparency through obstruction and scattering of light. Hence, large particle size greater than wavelength of light would cause greater obstruction. Another important factor that has been reported to affect light transmittance is the presence of non-starch material(s) in the matrix (Alimi & Workneh, 2018). Therefore, lower transparency reported for ASF could be due to its higher concentration of non-starch components with probably larger particle sizes in the film matrix.

Opacity is the opposite of transparency in definition (Santacruz et al., 2015), and the trends in this study were the same but in reverse direction. Since opacity is the opposite of transparency, presence of some components other than starch, such as lipids and proteins, would enhance it (Pelissari et al., 2013). These components were earlier mentioned in this study to affect strength of the films negatively.

Different products require different level of protection against light. Some food products require highly transparent films to expose their aesthetics during shelf display and enhance their acceptability by consumers. On the other hand, light sensitive products are better wrapped with opaque films.

Aside a (which software could not compare its means), there were significant ($p < .05$) differences in the values of other primary color parameters of the films (Table 1). The

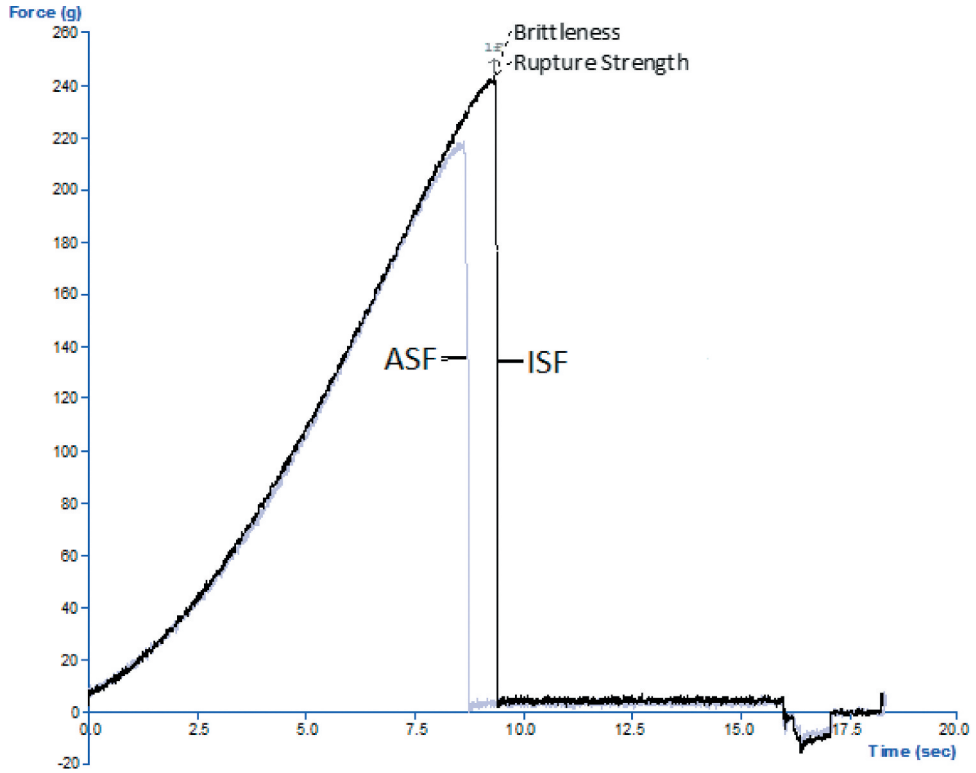

Figure 4. Force–time curves showing puncture force of *acha* and *iburu* starch films (ASF and ISF, respectively).

Figura 4. Curvas fuerza-tiempo que muestran la fuerza de punción de las películas de almidón de acha e iburu (ASF e ISF, respectivamente).

near zero negative values of "*a*" parameter for the films showed absence of red coloration, while positive *b* values indicated trace of yellowish coloration. Similar color trends were reported by Pelissari et al. (2013) for plantain banana films and Daudt et al. (2016) for *pinhão* starch films.

4. Conclusion

Films from *acha* (*Digitalia exilis*) and *iburu*(*Digitalia iburua*) starches exhibited good characteristics that could place them as potential coating and packaging materials for varying industrial uses. Scanning electron microscope pointed to the presence and magnitude of non-starch components in the films and the components were confirmed to be proteins, lipids and polyphenols by FTIR spectroscope. The comparative difference in the magnitude of the non-starch components in the films was found to be responsible for the variations in their functional, mechanical and photosensitive behaviors. The findings from this study are expected to guide on the potential applications of *acha* and *iburu* starch films as budding materials for different packaging and coating end uses.

Acknowledgments

Authors acknowledge the University of KwaZulu-Natal, South Africa for funding this research. The postdoctoral fellowship award provided for Dr. Buliyaminu Adegbemiro Alimi by the College of Agriculture, Engineering and Sciences, University of KwaZulu-Natal, South Africa is gratefully acknowledged.

Disclosure statement

No potential conflict of interest was reported by the author(s).

Funding

This work was supported by the Inyuvesi Yakwazulu-Natali [None].

References

Akman, P. K., Bozkurt, F., Dogan, K., Tornuk, F., & Tamturk, F. (2021). Fabrication and characterization of probiotic Lactobacillus plantarum loaded sodium alginate edible films. *Journal of Food Measurement and Characterization*, *15*(1), 84–92. https://doi.org/10.1007/s11694-020-00619-6

Alimi, B., Sibomana, M., Workneh, T., & Oke, M. (2017a). Some engineering properties of composite corn-banana custard flour. *Journal of Food Process Engineering*, *40*(3), e12444. https://doi.org/10.1111/jfpe.12444

Alimi, B. A., Shittu, T. A., & Sanni, L. O. (2014). Effect of hydrocolloids and egg content on sensory quality of coated fried yam chips. *Journal of Culinary Science and Technology*, *12*(2), 168–180. https://doi.org/10.1080/15428052.2014.880097

Alimi, B. A., & Workneh, T. S. (2018). Structural and physicochemical properties of heat moisture treated and citric acid modified *acha* and *iburu* starches. *Food Hydrocolloids*, *81*, 449–455. https://doi.org/10.1016/j.foodhyd.2018.03.027

Alimi, B. A., Workneh, T. S., & Oyeyinka, S. A. (2017b). Structural, rheological and in-vitro digestibility properties of composite corn-banana starch custard paste. *LWT-Food Science and Technology*, *79*, 84–91. https://doi.org/10.1016/j.lwt.2017.01.012

Alimi, B. A., Workneh, T. S., & Sibomana, M. S. (2016). Effect of hydrothermal modifications on functional, pasting and structural properties of false banana (*Ensete ventricosum*) starch. *Food Biophysics*, *11*(3), 248–256. https://doi.org/10.1007/s11483-016-9435-6

Andrade-Mahecha, M. M., Tapia-Blácido, D. R., & Menegalli, F. C. (2012). Development and optimization of biodegradable films based on achira flour. *Carbohydrate Polymers*, *88*(2), 449–458. https://doi.org/10.1016/j.carbpol.2011.12.024

Arezoo, E., Mohammadreza, E., Maryam, M., & Abdoreeza, M. N. (2020). The synergistic effecs of cinnamon essential oil and nano TiO_2 on antimicrobial and functional properties of sago starch films. *International Journal of Biological Macromolecules*, *157*, 743–751. https://doi.org/10.1016/j.ijbiomac.2019.11.244

Arueya, G. L., & Oyewale, T. M. (2015). Effect of varying degrees of succinylation on the functional and morphological properties of starch from acha (*Digitaria exilis* Kippis Stapf). *Food Chemistry*, *177*, 258–266. https://doi.org/10.1016/j.foodchem.2015.01.019

ASTM. (2018). *Standard test method for tensile properties of thin plastic sheeting D882-18. Annual book of ASTM standards*. American Society for Testing and Materials.

Batista, J. A., Tanada-Palmu, P. S., & Grosso, C. R. (2005). Efeito da adição de ácidos graxos em filmes à base de pectina. *Ciência E Tecnologia De Alimentos*, *25*(4), 781–788. https://doi.org/10.1590/S0101-20612005000400025

Bergo, P., Sobral, P. J. A., & Prison, J. M. (2010). Effect of glycerol on physical properties of cassava starch films. *Journal of Food Processing and Preservation*, *34*(s2), 401–410. https://doi.org/10.1111/j.1745-4549.2008.00282.x

Bourtoom, T., & Chinnan, M. S. (2008). Preparation and properties of rice starch–chitosan blend biodegradable film. *LWT-Food Science and Technology*, *41*(9), 1633–1641. https://doi.org/10.1016/j.lwt.2007.10.014

Dang, K. M., & Yoksan, R. (2016). Morphological characteristics and barrier properties of thermoplastic starch/chitosan blown film. *Carbohydrate Polymers*, *150*, 40–47. https://doi.org/10.1016/j.carbpol.2016.04.113

Daudt, R. M., Avena-Bustillos, R. J., Williams, T., Wood, D. F., Külkamp-Guerreiro, I. C., Marczak, L. D. F., & McHugh, T. H. (2016). Comparative study on properties of edible films based on pinhão (*Araucaria angustifolia*) starch and flour. *Food Hydrocolloids*, *60*, 279–287. https://doi.org/10.1016/j.foodhyd.2016.03.040

Gutiérrez, T. J., Tapia, M. S., Pérez, E., & Famá, L. (2015). Structural and mechanical properties of edible films made from native and modified cush-cush yam and cassava starch. *Food Hydrocolloids*, *45*, 211–217. https://doi.org/10.1016/j.foodhyd.2014.11.017

Hizukuri, S., Kaneko, T., & Takeda, Y. (1983). Measurement of the chain length of amylopectin and its relevance to the origin of crystalline polymorphism of starch granules. *Biochimica et Biophysica Acta (BBA)-General Subjects*, *760*(1), 188–191. https://doi.org/10.1016/0304-4165(83)90142-3

Jafarzadeh, S., Jafari, S. M., Salehabadi, A., Nafchi, A. M., Uthaya, U. S., & Khalil, H. A. (2020). Biodegradable green packaging with antimicrobial functions based on the bioactive compounds from tropical plants and their by-products. *Trends in Food Science and Technology*, *1000*, 262–277. https://doi.org/10.1016/j.tifs.2020.06.017

Jideani, I. A., & Jideani, V. A. (2011). Developments on the cereal grains *Digitaria exilis* (acha) and *Digitaria iburua* (iburu). *Journal of Food Science and Technology*, *48*(3), 251–259. https://doi.org/10.1007/s13197-010-0208-9

Kampeerapappun, P., Aht-ong, D., Pentrakoon, D., & Srikulkit, K. (2007). Preparation of cassava starch/montmorillonite composite film. *Carbohydrate Polymers*, *67*(2), 155–163. https://doi.org/10.1016/j.carbpol.2006.05.012

Kizil, R., Irudayaraj, J., & Seetharaman, K. (2002). Characterization of irradiated starches by using FT-Raman and FTIR spectroscopy. *Journal of Agriculture and Food Chemistry*, *50*(14), 3912–3918. https://doi.org/10.1021/jf011652p

Liu, X., Yang, Y. J., & Wang, Z. W. (2018). Structure characteristics of Coix seeds prolamins and physicochemical and mechanical properties of their films. *Journal of Cereal Science*, *79*, 233–239. https://doi.org/10.1016/j.jcs.2017.11.002

Mei, L. X., Nafchi, A. M., Ghasemipour, F., Easa, A. M., Jafarzadeh, S., & Al-Hassan, A. A. (2020). Characteruzation of pH sensitive sago starch films enriched with anthocyanin-rich torch ginger extract. *International Journal of Biological Macromolecules*, *164*, 4603–4612. https://doi.org/10.1016/j.ijbiomac.2020.09.082

Müller, C. M., Yamashita, F., & Laurindo, J. B. (2008). Evaluation of the effects of glycerol and sorbitol concentration and water activity on the water barrier properties of cassava starch films through

a solubility approach. *Carbohydrate Polymers*, *72*(1), 82–87. https://doi.org/10.1016/j.carbpol.2007.07.026

Pelissari, F. M., Andrade-Mahecha, M. M., Do Amaral Sobral, P. J., & Menegalli, F. C. (2013). Comparative study on the properties of flour and starch films of plantain bananas (*Musa paradisiaca*). *Food Hydrocolloids*, *30*(2), 681–690. https://doi.org/10.1016/j.foodhyd.2012.08.007

Santacruz, S., Rivadeneira, C., & Castro, M. (2015). Edible films based on starch and chitosan. Effect of starch source and concentration, plasticizer, surfactant's hydrophobic tail and mechanical treatment. *Food Hydrocolloids*, *49*, 89–94. https://doi.org/10.1016/j.foodhyd.2015.03.019

Sanyang, M. L., Sapuan, S. M., Jawaid, M., Ishak, M. R., & Sahari, J. (2016). Development and characterization of sugar palm starch and poly (lactic acid) bilayer films. *Carbohydrate Polymers*, *146*, 36–45. https://doi.org/10.1016/j.carbpol.2016.03.051

Shaili, T., Abdorreza, M. N., & Fariborz, N. (2015). Functional, thermal and antimicrobial properties of soluble soybean polysaccharide biocomposites reinforced by nano TiO_2. *Carbohydrate Polymers*, *134*, 726–731. https://doi.org/10.016/j.carbpol.2015.08.075

Shittu, T. A., Jayaramudu, J., Sivakumar, D., & Sadiku, E. R. (2014). Physicochemical and engineering properties of nanocomposite films based on chitosan and pseudoboehmite alumina. *Food and Bioprocess Technology*, *7*(8), 2423–2433. https://doi.org/10.1007/s11947-014-1305-y

Van Soest, J. J., Tournois, H., De Wit, D., & Vliegenthart, J. F. (1995). Short-range structure in (partially) crystalline potato starch determined with attenuated total reflectance Fourier-transform IR spectroscopy. *Carbohydrate Research*, *279*, 201–214. https://doi.org/10.1016/0008-6215(95)00270-7

Yildirim-Yalçin, M., Şeker, M., & Sadikoğlu, H. (2019). Development and characterization of edible films based on modified corn starch and grape juice. *Food Chemistry*, *292*, 6–13. https://doi.org/10.1016/j.foodchem.2019.04.006

Zhang, Y., & Han, J. H. (2006). Plasticization of pea starch films with monosaccharides and polyols. *Journal of Food Science*, *71*(6), E253–E261. https://doi.org/10.1111/j.1750-3841.2006.00075.x